Pflugers Arch - Eur J Physiol
DOI 10.1007/s00424-016-1880-z

SIGNALING AND CELL PHYSIOLOGY

Molecular mechanisms underlying inhibition of STIM1-Orai1-mediated Ca^{2+} entry induced by 2-aminoethoxydiphenyl borate

Ming Wei[1] · Yandong Zhou[2] · Aomin Sun[1] · Guolin Ma[3] · Lian He[3] · Lijuan Zhou[1] · Shuce Zhang[1] · Jin Liu[1] · Shenyuan L. Zhang[4] · Donald L. Gill[2] · Youjun Wang[1]

Received: 22 June 2016 / Revised: 24 August 2016 / Accepted: 7 September 2016

Abstract Store-operated Ca^{2+} entry (SOCE) mediated by STIM1 and Orai1 is crucial for Ca^{2+} signaling and homeostasis in most cell types. 2-Aminoethoxydiphenyl borate (2-APB) is a well-described SOCE inhibitor, but its mechanisms of action remain largely elusive. Here, we show that 2-APB does not affect the dimeric state of STIM1, but enhances the intramolecular coupling between the coiled-coil 1 (CC1) and STIM-Orai-activating region (SOAR) of STIM1, with subsequent reduction in the formation of STIM1 puncta in the absence of Orai1 overexpression. 2-APB also inhibits Orai1 channels, directly inhibiting Ca^{2+} entry through the constitutively active, STIM1-independent Orai1 mutants, Orai1-P245T and Orai1-V102A. When unbound from STIM1, the constitutively active Orai1-V102C mutant is not inhibited by 2-APB. Thus, we used Orai1-V012C as a tool to examine whether 2-APB can also inhibit the coupling between STIM1 and Orai1. We reveal that the functional coupling between STIM1 and Orai1-V102C is inhibited by 2-APB. This inhibition on coupling is indirect, arising from 2-APB's action on STIM1, and it is most likely mediated by functional channel residues in the Orai1 *N*-terminus. Overall, our findings on this two-site inhibition mediated by 2-APB provide new understanding on Orai1-activation by STIM1, important to future drug design.

Keywords STIM1 · Orai1 · SOCE · 2-APB · Puncta · FRET · Calcium

Ming Wei, Yandong Zhou, and Aomin Sun contributed equally to this work.

✉ Donald L. Gill
dgill4@hmc.psu.edu

✉ Youjun Wang
wyoujun@bnu.edu.cn

[1] Beijing Key Laboratory of Gene Resources and Molecular Development, College of Life Sciences, Beijing Normal University, Beijing 100875, People's Republic of China

[2] Department of Cellular and Molecular Physiology, The Pennsylvania State University College of Medicine, Hershey, PA 17033, USA

[3] Institute of Biosciences and Technology, Texas A&M University Health Science Center, Houston, TX 77030, USA

[4] Department of Medical Physiology, College of Medicine, Texas A&M University Health Science Center, Temple, TX 76504, USA

Introduction

As a universal second messenger, Ca^{2+} mediates control over a wide spectrum of cellular activities [5, 8]. In most cell types, store-operated Ca^{2+} entry (SOCE) is an important Ca^{2+} influx process mediating both Ca^{2+} signaling and homeostasis [26, 35, 46, 52]. Stromal interaction molecule (STIM) proteins and Orai channels are the two essential and sufficient mediators of SOCE. The endoplasmic reticulum (ER) membrane STIM proteins function as Ca^{2+} sensors that can respond to decreased ER luminal Ca^{2+}, and Orai channels are STIM-targeted, highly selective Ca^{2+} channels in the plasma membrane [16]. STIM and Orai mediate Ca^{2+} signals in many immune, vascular, and contractile cell types and are implicated in a range of immune deficiency diseases and cancer [3, 35, 46, 49, 50]. Much important information regarding the molecular mechanisms that lead to Orai1 activation has been obtained recently [17, 24, 34, 45, 46], yet the exact nature of its coupling and activation process still awaits further clarification.

Obviously, the discovery and design of pharmacological tools targeting the STIM/Orai signaling process is crucial to dissect the underlying molecular mechanism of SOCE and to more thoroughly examine its physiological or pathological

Published online: 10 October 2016

roles, in potential disease therapy. So far, many modifiers of SOCE have been found [48]. However, most of these available inhibitors have flaws and fail in one or more of the following criteria: avidity, specificity, rapidity of action, and reversibility (reviewed in [19, 41]). One hindrance in developing better pharmacological tools is the lack of understanding of the currently available inhibitors. As one of the most characterized modulators of SOCE, 2-aminoethoxydiphenyl borate (2-APB) has been shown to enhance SOCE activity at lower levels (5–10 μM) yet rapidly block it at 50 μM [10, 22, 25, 38, 39, 43, 53]. However, the molecular basis for its actions on SOCE remains largely elusive.

In this study, we aim to dissect the underlying molecular mechanisms of SOCE inhibition by 2-APB at 50 μM. Our results show that, in addition to its direct inhibition on Orai1 channels, 2-APB can also directly inhibit the STIM1 protein by enhancing intramolecular interactions between the CC1 and SOAR region of STIM1. This inhibition on STIM1 leads to the reduction of STIM1 puncta formation in native HEK293 cells with endogenous levels of Orai1. 2-APB did not directly inhibit the coupling between STIM1 and Orai1, while its actions on STIM1 may lead to an indirect inhibition on STIM1-mediated gating of Orai1.

Methods

DNA constructs, cell culture, and transfection

Cyan fluorescent protein (CFP)-Orai1-V102C was generated from CFP-Orai1 by PolePolar Biotechnology Co., Ltd (Beijing, China). Truncations of CFP-Orai1-V102C-ΔC2 (ΔT266-A301) and CFP-Orai1-V102C-ΔN2 (ΔM1-K85) were then correspondingly generated from CFP-Orai1-V102C by the same company. Orai1-V102A-CFP was generated from Orai1-CFP by TransGen Biotech (Beijing, China). Orai1-K85E-V102C-CFP, CFP-Orai1-V102A-ΔC2, and CFP-Orai1-V102A were made by point mutations from corresponding Orai1 or the Orai1-V102C mutant (TransGen Biotech, Beijing, China). Orai1-P245T-CFP was made from Orai1-CFP using the QuikChange Lightning site-directed mutagenesis kit (Agilent).

Cell culture and generation of stable cell lines, wild-type Human embryonic kidney 293 (HEK wt) cells, were maintained in regular DMEM (HyClone) supplemented with 10 % FBS (Cleson Scientific) and penicillin and streptomycin (Thermo Scientific) at 37 °C with 5 % CO_2 as previously described [14]. HEK cells stably expressing Orai1-V102C-CFP and STIM1-yellow fluorescent protein (YFP) were generated by electroporation using the pIRES-Orai1-V102-CFP or MO91-STIM1-YFP constructs and then selected with 100 μg/ml G418 (Invitrogen) or 2 μg/ml puromycin (Invitrogen) correspondingly [14]. HEK stable cells co-expressing STIM1-YFP and Orai1-CFP or Orai1-V102C-CFP cells were generated by introducing STIM1-YFP into Orai1-CFP or Orai1-V102C-CFP stable cells using similar protocols. For HEK stable cells expressing Orai1 or Orai1-V102C, they were maintained in the abovementioned medium supplemented with 100 μg/ml G418; for HEK STIM1-YFP cells, the extra supplement is 2 μg/ml puromycin; for stable cells co-expressing two proteins, both puromycin and G418 were added in the culture medium.

Transient transfections was undertaken with polyethylenimine (PEI, Polysciences, Inc., cat. no. 23966) [6] following the manufacturer's protocol. The DNA to PEI ratio used was 1:2, 1 day after cells were seeded on a 25-mm round coverslip at 70 % confluence. All imaging experiments were performed 1 or 2 days after transfection.

Single-cell intracellular Ca^{2+} measurements

Intracellular Ca^{2+} signals measured by Fura-2 indicator were recorded using a ZEISS Observer A1 microscope equipped with a Lambda DG-4 light source (Sutter Instruments), BrightLine FURA2-C-000 filter set (Semrock Inc), a ×40 oil objective (NA = 1.30), an iXon3 EMCCD camera (Oxford Instruments), and the MetaFluor software (Molecular Devices).

Protocols for the loading of Fura-2-acetoxymethyl ester (AM) were similar to those described previously [24]: HEK293 cells were first placed in the imaging solution with 1 mM $CaCl_2$ and 2 μM Fura-2 AM for 30 min. Next, cells were placed in Fura-2 AM free imaging solution with 1 mM $CaCl_2$ for another 30 min. Collection of Fura-2 signals was as follows: emission fluorescence at 509 nm generated by 340-nm excitation light (F_{340}) and 380-nm light (F_{380}) was collected every 2 s, and intracellular Ca^{2+} levels are shown as F_{340}/F_{380} ratio.

The imaging solution consisted of 107 mM NaCl, 7.2 mM KCl, 1.2 mM $MgCl_2$, 11.5 mM glucose, and 20 mM HEPES-NaOH (pH 7.2). Depending on the specific design of each experiment, different amounts of $CaCl_2$ and other types of reagents were also included in the imaging solution. For cells transfected with constructs that give rise to constitutive Ca^{2+} influx, either 1 mM Ca^{2+} with 10 μM $GdCl_3$, 100~300 μM Ca^{2+}, or nominally Ca^{2+}-free solution were used to keep cells healthy. All experiments were carried out at room temperature. Traces shown are representative of at least three independent repeats with each including 15–60 single cells.

Fluorescence and Förster resonance energy transfer imaging

For Förster resonance energy transfer (FRET) measurements, necessary calibrations and off-line analysis were performed as described before [24, 32, 58]. Briefly, raw images (F_{CFP}, F_{YFP},

and F_{raw}, respectively) were collected every 10 s using the abovementioned imaging system equipped with an Optosplit II Image Splitter (Cairn Research Ltd.) and the following three filters: CFP ($428.9 \pm 5.5_{Ex}/465 \pm 32_{Em}$), YFP ($502.6 \pm 11.2_{Ex}/549 \pm 21_{Em}$), and $FRET_{raw}$ ($428.9 \pm 5.5_{Ex}/549 \pm 21_{Em}$). After readings from raw images were obtained, the three-channel-corrected FRET was first calculated using this formula: $FRET_c = F_{raw} - F_d/D_d \times F_{CFP} - F_a/D_a \times F_{YFP}$, where $FRET_c$ represents the corrected total amount of energy transfer, F_d/D_d represents measured bleed-through of CFP into the FRET filter (0.84), and F_a/D_a represents measured bleed-through of YFP through the FRET filter (0.13). Normalized FRET (N-FRET) was calculated by normalizing $FRET_c$ values against donor fluorescence (F_{CFP}) to reduce variations caused by differences in expression levels. The system-independent apparent FRET efficiency, E_{app}, was calculated using the following equation: E_{app} = N-FRET / (N-FRET + G), where G (4.59) is the system-dependent factor and was obtained with the same protocol as described previously [58]. YFP-STIM1-D76G-F394H-CFP expressed in HEK293 cells was used as a calibrator of relative expression levels of CFP- and YFP-tagged proteins. Also, it served as a negative control in our experiments, since YFP and CFP on this probe are separated by the ER membrane with a distance more than 10 nm [7]. To minimize fluctuations in E_{app} caused by variations in expression ratios of donor protein to acceptor protein, only cells with F_{CFP}/F_{YFP} ratio falling between 0.5 and 1 were used for data analysis. All fluorescence images were collected and processed with MetaFluor software (Molecular Devices), and the resulting data were further analyzed with Matlab R2012b software and plotted with Prism5 software. Representative traces of at least three independent experiments are shown as mean ± SEM.

Unless specified, fluorescence images or figures showing cellular distribution of E_{app} were obtained with a ZEISS Observer Z1 fluorescence microscope controlled by Zen Software. CFP and YFP images were collected with a ×40 oil objective (N.A. 1.3) and corresponding Semrock BrightLine filter sets (CFP-2432C-000, YFP-2427B-000). A re-combination of the above filter sets was used to collect raw FRET images, with the excitation filter from the CFP filter set, while the dichroic and emission filters were from the YFP filter set. Cellular E_{app} images were generated by executing a ZEISS-made macro in Zen software using the same calibration methods and the following parameters: $F_d/D_d = 0.37$, $F_a/D_a = 0.18$, and G = 2.94.

Confocal microscopy and puncta analysis

Images from some experiments examining co-localization between proteins or STIM1 puncta were taken with a ZEISS LSM700 confocal microscope equipped with ×100 oil objective (N.A. 1.6), 405- and 488-nm laser, controlled by Zen software.

To calibrate bleed-through between different channels, besides cells co-expressing both YFP- and CFP-tagged proteins, fluorescence images of cells expressing only either CFP- or YFP-tagged proteins were also collected with the same parameters as those used for co-expressing cells. The bleed-through factors were calculated off-line with ImageJ software. The co-localization images shown were bleed-through-corrected.

Puncta analysis was done with a customized macro plug-in of ImageJ software modified from a previously published protocol [15]. Briefly, puncta images were first converted from 16 to 8 bits, and then background was subtracted using a rolling ball with a radius larger than 15 pixels. The resulting images were converted to binary images and then further treated with "watershed" function. Statistics of puncta were then obtained with "Analyze particles" function in ImageJ. Only particles with a size larger than 4 pixels were taken as puncta. The macro file used for puncta analysis is available upon request.

Electrophysiology

Electrophysiological measurements were undertaken with conventional whole-cell patch clamp using cells grown on glass coverslips as described previously [51]. After the establishment of the whole-cell configuration, a holding potential of 0 mV were applied. A 50-ms step to −100 mV followed by a 50-ms ramp spanning from −100 to +100 mV were delivered at a rate of 0.5 Hz. The pipette solution contained 145 mM CsGlu, 10 mM HEPES, 10 mM EGTA, 8 mM NaCl, 6 mM $MgCl_2$, and 2 mM Mg-ATP (pH 7.2). Eight millimolars of Mg^{2+} and ATP was used to inhibit TRPM7 current. For experiments performed in Orai1-V102C stable cells, 3 mM $CaCl_2$ was added into pipette solution to make the free Ca^{2+} concentration at 100 nM. The extracellular solutions contained 145 mM NaCl, 10 mM $CaCl_2$, 10 mM CsCl, 2 mM $MgCl_2$, 2.8 mM KCl, 10 mM HEPES, and 10 mM glucose (pH 7.4). A 10-mV junction potential compensation was applied.

Results

2-APB enhances interactions between STIM1-CC1 and SOAR, which is essential and sufficient for its inhibition on STIM1 puncta formation

When ER Ca^{2+} stores are full, STIM1 molecules are uniformly distributed over the entire ER membrane. Upon store depletion, STIM1 forms puncta and activates Orai1 channels [46]. High concentration (50 μM) of 2-APB, a powerful SOCE modifier, can block or reverse the formation of STIM1 puncta, and it was proposed that such reduction of

puncta mediated the inhibition on SOCE [10, 38]. However, the exact mechanisms by which 2-APB affects puncta are still not known. We addressed this question by examining the effects of 2-APB on several known critical steps involved in the formation of STIM1 puncta.

Initially, we tested whether 2-APB has any effect on STIM1-STIM1 interactions. Following store depletion, the dissociation of Ca^{2+} ions from the EF hand within the STIM1 ER-luminal region triggers dimerization of the luminal domain [47]. Thus, we examined FRET signals between the C-terminally truncated STIM1-(1–237) fragment [24] containing the entire ER-luminal and TM region of STIM1. Our results revealed that 2-APB had no effect on FRET signals between CFP- and YFP-tagged versions of these STIM1 fragments, regardless of whether the ER store was full or depleted (Fig. 1a). These results indicate that 2-APB does not affect the dimeric state of the entire ER and TM regions of STIM1. Next, we examined whether interactions between STIM1 cytosolic fragments were affected by 2-APB. The entire cytosolic C-terminal domain (STIM1ct), or just the STIM1-Orai1-activating region (SOAR) or CRAC-activating domain (CAD) of STIM1, each exist as cytosolic dimers when expressed (reviewed in [46]). Indeed, the SOAR/CAD region of STIM1 is essential for oligomerization and puncta formation of STIM1 [9, 12]. Our results show that 2-APB does not induce any significant changes in FRET signals between STIM1ct (Fig. 1b) or SOAR molecules (Fig. 1c), regardless of whether FRET signals were measured when they were Orai1-bound or free in the cytosol (Fig. 1c). Thus, 2-APB does not directly alter cytosolic STIM1-STIM1 interactions. 2-APB also did not have any effect on FRET signals between YFP-STIM1 and CFP-STIM1 (Fig. 1d). Together, these results indicate that 2-APB does not inhibit STIM1 puncta by disrupting intermolecular interactions of STIM1.

We then examined whether 2-APB can block the intramolecular interactions that occur during STIM1 activation using a two-component system consisting of STIM1-(1–310)-CFP and YFP-SOAR. This two-component system has been successfully applied to report interactions between STIM1-CC1 and SOAR using co-localization or FRET imaging [24]. We tested the effects of 2-APB on the coupling of STIM1-CC1 and SOAR with this system. When co-expressed in HEK cells, STIM1-(1–310)-CFP and YFP-SOAR co-localize (Fig. 1e, top row) and have high FRET signals at rest (Fig. 1h). Upon store depletion with ionomycin, SOAR was uncoupled from ER-localized STIM1-(1–310) and became evenly distributed in the cytosol (Fig. 1e, middle row)), resulting in diminished FRET signals (Fig. 1h). After the application of 50 μM 2-APB, SOAR moved back to the ER and co-localized with STIM1-CC1 again (Fig. 1e, bottom row). As a result, the ionomycin-induced decrease in FRET signal was partially reversed by 2-APB (Fig. 1h). These results indicate that 2-APB can induce coupling between STIM1-CC1 and SOAR, and the enhanced coupling between STIM1-CC1 and SOAR can partially recover the FRET decrease caused by store depletion. Therefore, 2-APB can induce or enhance interactions between STIM1-CC1 and SOAR, locking STIM1 into its resting, inhibitory state.

To test whether those critical residues, essential for interactions between STIM1-CC1 and SOAR, are also required for 2-APB's actions on puncta, we examined 2-APB's effects on interactions between corresponding mutants of STIM1-(1–310) or SOAR. Both STIM1-(1–310)-L258G or SOAR-L416G mutations have been previously shown to disrupt interactions between STIM1-CC1 and SOAR [24] (Fig. 1f, g). When examined with co-localization imaging, 2-APB also failed to dock SOAR-L416G back to ER-localized STIM1-CC1 (Fig. 1f) or restore the docking of SOAR back to STIM1-(1–310)-L258G (Fig. 1g). These mutants also abolished 2-APB's ability to restore FRET signals between SOAR and STIM1-(1–310) (Fig. 1h). These results reveal that 2-APB's actions on STIM1 require those critical residues that are essential for the coupling between STIM1-CC1 and SOAR.

To test whether the enhanced coupling between STIM1-CC1 and SOAR is sufficient for the inhibition of puncta formation by 2-APB, we examined the effects of 2-APB on puncta formed by STIM1 and various mutants (Fig. 2a, b). Similar to previous reports [10, 38], 2-APB can reduce puncta formed by wt STIM1 after store depletion (Fig. 2a, top row). 2-APB did not significantly reduce the number of puncta (Fig. 2b, upper); it reduced the average size of puncta instead (Fig. 2b, lower). The D76A mutation in the EF hand of STIM1 causes the loss of Ca^{2+} binding, resulting in the formation of constitutive puncta [15] (Fig. 2a, 2nd row). Application of 50 μM 2-APB could largely inhibit puncta of YFP-STIM1-D76A. However, constitutive puncta formed by STIM1-L258G (Fig. 2a, third panel from top) or STIM1-L416G (Fig. 2a, bottom panel) were unaffected by 2-APB. Therefore, 2-APB's inhibitory effect on STIM1 puncta is dependent on residues critical for interactions between STIM1-CC1 and SOAR. The enhanced interactions between STIM1-CC1 and SOAR (residue 344–442) are essential and sufficient for 2-APB's inhibition on STIM1 puncta.

2-APB's inhibitory effect on STIM1 is not essential for the inhibition of SOCE

2-APB inhibits SOCE at high concentrations [19, 41], and the disruption of STIM1 puncta by 2-APB was proposed to explain its inhibition on Ca^{2+} influx through Orai1 channels [38]. However, there have been some discrepancies regarding 2-APB's ability to inhibit STIM1 puncta [10, 32, 59]. We thus examined whether the inhibition of puncta and of SOCE represent the same mechanism or can be separated. We examined this by comparing 2-APB's effects on SOCE and puncta in

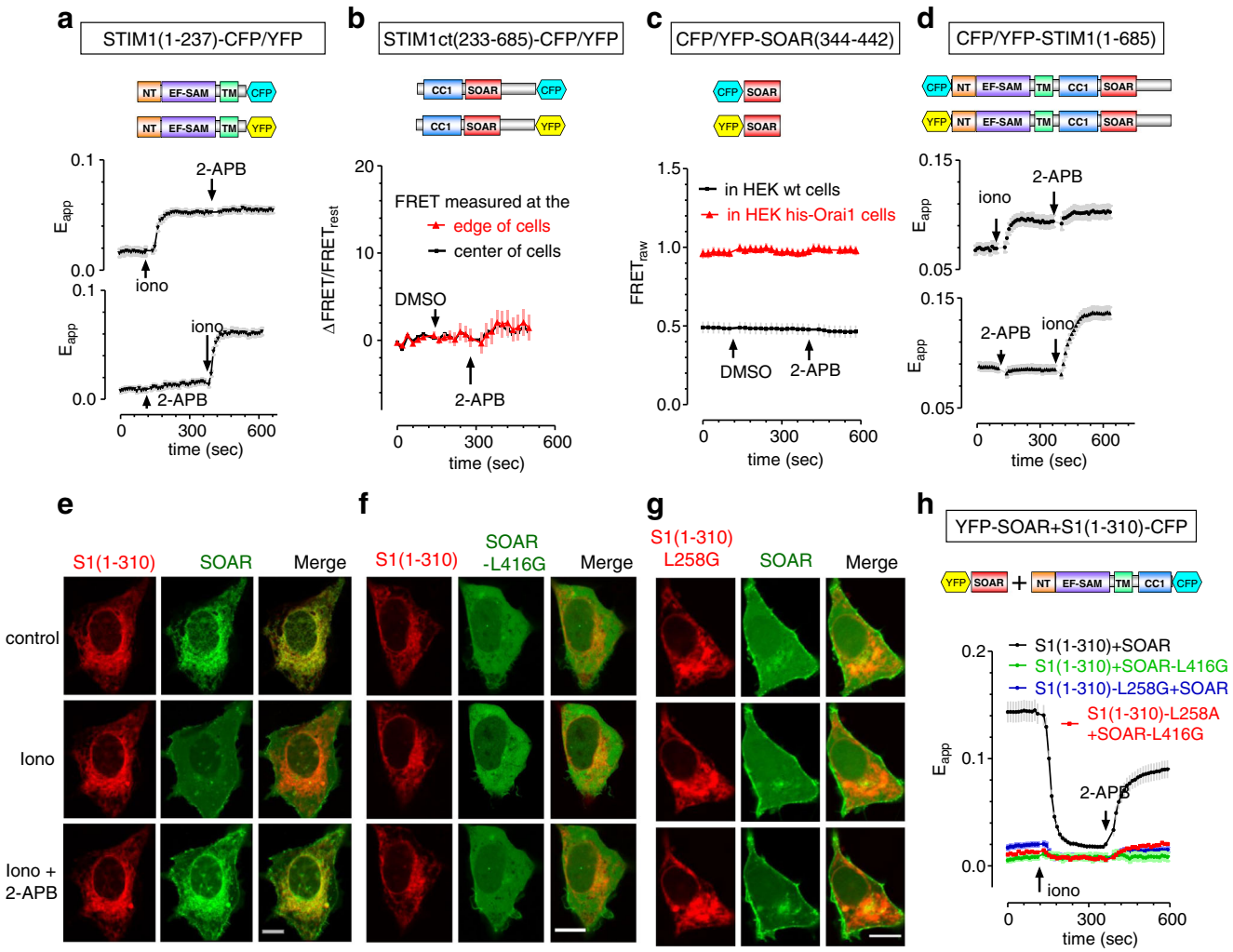

Fig. 1 2-APB has no effect on STIM1-STIM1 interactions, but enhanced intramolecular interactions between STIM1-CC1 and SOAR region. **a** In HEK wt cells transiently co-expressing STIM1-(1–237)-CFP or STIM1-(1–237)-YFP, 2-APB did not induce detectable changes in FRET signals between the two proteins regardless of store status. *Upper trace*: 2-APB (50 μM) was applied after ionomycin. *Lower trace*: 2-APB was applied before ionomycin (2.5 μM). **b** 2-APB did not induce any detectable changes in FRET signals between STIM1ct-YFP and STIM1ct-CFP that were transiently co-expressed in HEK wt cells. **c** 2-APB had no effect on FRET signals between YFP- and CFP-SOAR transiently co-expressed in HEK wt or his-Orai1 cells. **d** In HEK wt cells transiently co-expressing YFP-STIM1 or CFP-STIM1, ionomycin-induced FRET changes were unaffected by 2-APB, regardless of whether it was applied after ionomycin (upper figure) or before store depletion (bottom figure). **e**–**h** Using HEK wt cells co-expressing STIM1-(1–310)-CFP and YFP-SOAR or their corresponding mutants, after ER Ca^{2+} stores were depleted with ionomycin (2.5 μM), effects of 2-APB (50 μM) on these STIM1 mutants were tested. *Images* shown here were collected with confocal imaging (*scale bar*, 10 μm). **e** 2-APB partially reversed the ionomycin-diminished co-localization between STIM1-(1–310) and SOAR. **f** STIM1-L416G lost its ability to co-localize with STIM1-(1–310), and 2-APB cannot make STIM1-L416G co-localize with STIM1-(1–310). **g** Similarly, STIM1-(1–310)-L258G mutant abolished ionomycin- or 2-APB-induced changes in co-localizations between STIM1-(1–310)-L258G and SOAR. **h** The effects of ionomycin or 2-APB on the FRET signals between STIM1-(1–310)-CFP and YFP-SOAR or their corresponding mutants were examined. 2-APB could partially reverse the ionomycin-induced decreases in FRET signals between wt STIM1-(1–310) and wt SOAR. STIM1-(1–310)-L258G or SOAR-L416 abolished these effects induced by ionomycin or 2-APB. At least three independent repeats were conducted, and typical traces or images are shown here

HEK wt cells expressing STIM1 or mutants thereof (Fig. 2a–c). In cells expressing either wt STIM1 or STIM1-D76A, both of which retain intact CC1-SOAR interactions, 2-APB reduced the punctate area similarly (Fig. 2a, top two rows). 2-APB did not inhibit puncta formed by the STIM1-L258G or STIM1-L416G mutants with no CC1-SOAR interactions (Fig. 2a, bottom two panels). However, whether STIM1 puncta were inhibited or not, SOCE was inhibited similarly in all groups (Fig. 2c). Therefore, 2-APB's action on STIM1 puncta and its inhibitory effect on SOCE can be separated in HEK wt cells overexpressing STIM1 or its mutants.

We also directly compared the effects of 2-APB on STIM1 puncta and SOCE in cells with or without co-expression of Orai1 channels. We performed these experiments with two

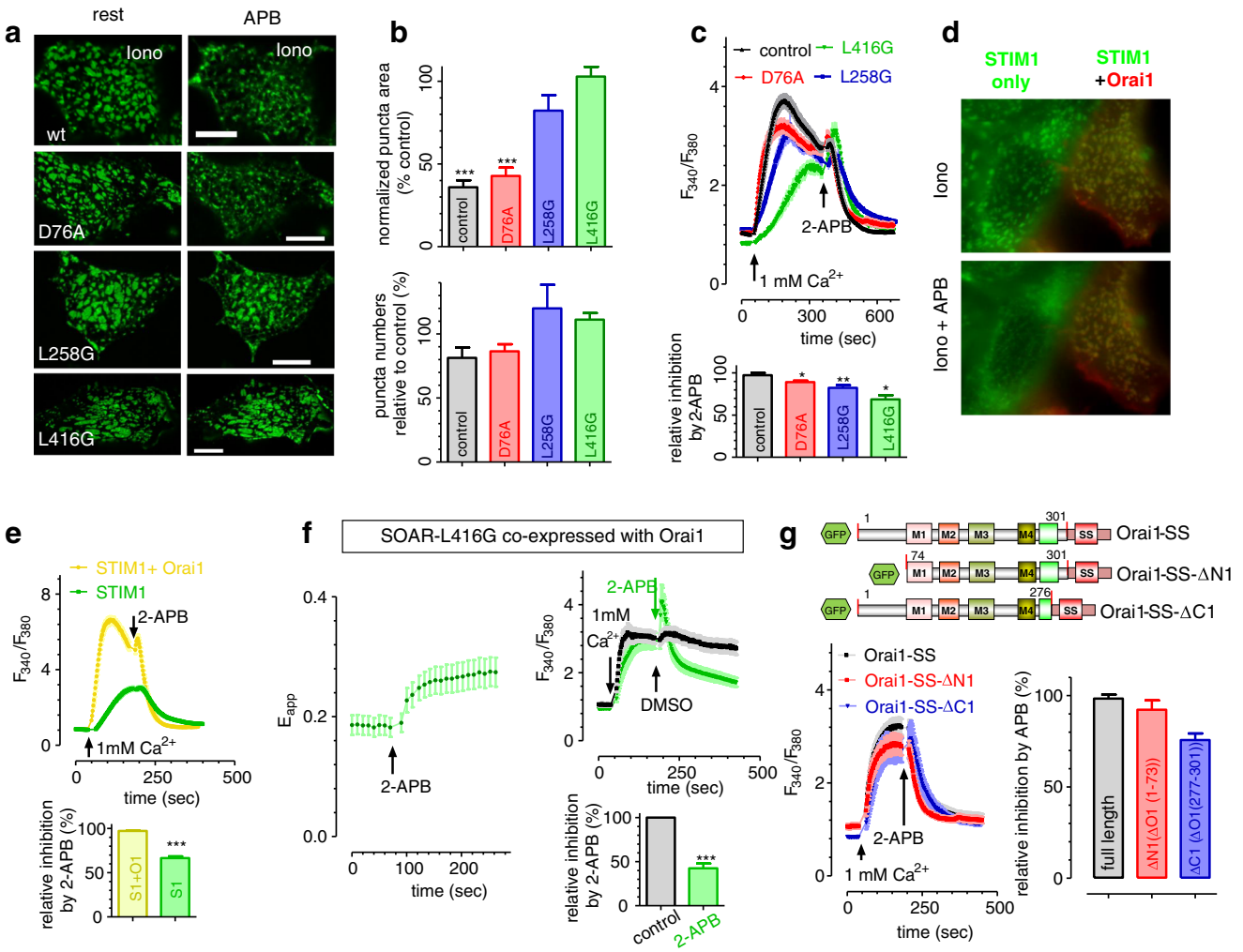

Fig. 2 After abolishing its inhibitory effect on STIM1 or STIM1 puncta, 2-APB can still inhibit Ca^{2+} influxes that are mediated by various types of STIM1/Orai1 complexes**.** Intracellular Ca^{2+} signals were measured with Fura-2, a ratio metric Ca^{2+} indicator. **a**–**c** In HEK wt cells transiently expressing wt STIM1 or its various mutants (wt STIM1, STIM1-D76A, STIM1-L258G, or STIM1-L416G), 2-APB's effects on ionomycin-induced or constitutive puncta (**a**, **b**) or corresponding Ca^{2+} influx (**c**) were examined. **a** Punctate images taken with confocal microscopy. Puncta formed by wt STIM1 or STIM1-D76A were both inhibited by 2-APB, while constitutive puncta formed by STIM1-L258G or STIM1-L416G were not significantly affected. (*Scale bar* 10 μm). **b** Statistics of figure (**a**), with the control condition before adding 2APB as 100 %. *Top image*: effects on puncta number ($p > 0.06$, paired *t* test, $n \geq 6$). *Bottom image*: effect of 2-APB on mean punctate area (*** paired *t* test, $p < 0.001$). **c** 2-APB inhibited Ca^{2+} influxes similarly in cells expressing wt STIM1 or different STIM1 mutants. *Upper image*, representative traces; *lower image*, statistics showing the APB-induced inhibition relative to DMSO controls (*t* test, $p < 0.03$, $n = 3$). **d**, **e** Two types of stable cells were seeded on the same coverslip: HEK stable cells co-expressing just STIM1-YFP (*green*), or both STIM1-YFP and Orai1-CFP (*orange*), and the effects of 2-APB on STIM1-puncta (**d**) or SOCE (**e**) were examined. **d** Relative to before control (100 %), 2-APB significantly reduced the punctate area to 36.0 ± 5.5 % in STIM1 cells ($p < 0.001$, paired *t* test), while it has no effect on punctate area in HEK STIM1-Orai1 cells (the *orange cell* in *left figure*) (108.4 ± 5.3 %, $p > 0.17$, paired *t* test). $n = 3$, at least six cells were analyzed for each repeat. Images were obtained with regular epifluorescence microscopy. **e** 2-APB inhibits SOCE in both STIM1 cells and STIM1-Orai1 cells. Cells were pre-treated with 2.5 μM ionomycin for 5 min before recording. *Upper image*, representative traces; *lower image*, statistics showing the APB-induced inhibition relative to DMSO controls (*t* test, $p < 0.001$, $n = 3$). **f** In HEK Orai1-CFP cells transiently expressing YFP-SOAR-L416G, 2-APB increased the FRET signals (*left figure*), but inhibited the Ca^{2+} entry (*upper right figure*), even though both processes are mediated by these two proteins. *Lower right image*, statistics showing the APB-induced inhibition relative to DMSO controls (*t* test, $p < 0.001$, $n = 3$). **g** In HEK wt cells transiently expressing eGFP-Orai1-SS, or its corresponding ΔN1(Δ1–73), ΔC1(Δ277–301) mutants. Constitutive Ca^{2+} entry was similarly inhibited by 2-APB. *Left*, typical traces; *right*, statistics showing the APB-induced inhibition relative to DMSO controls (*t* test, $p < 0.001$, $n = 3$). (Color figure online)

types of cells seeded on the same coverslip: cells overexpressing STIM1-YFP only, or cells co-expressing both STIM1-YFP and Orai1-CFP. In STIM1-YFP cells, 2-APB greatly reduced the punctate area of STIM1 (Fig. 2d, "green" cell on the left). However, in STIM1-YFP-Orai1-CFP double-expressing cells, STIM1 puncta were unaffected by 2-APB (Fig. 2d, "orange" cell on the right). This result indicates that Orai1-coupling with STIM1 can prevent the inhibitory effect

of 2-APB on STIM1 puncta. 2-APB's failure to inhibit STIM1 puncta in STIM1-Orai1 cells may be due to its enhancing effects on the coupling between STIM1ct and Orai1 [53]. Even though 2-APB's ability to reduce STIM1 puncta is abolished in HEK STIM1-Orai1 cells, it could still greatly inhibit SOCE (Fig. 2e). Therefore, the inhibition of SOCE can clearly be separated from the disruption of STIM1 puncta in cells co-expressing Orai1.

Overall, with either co-expression of Orai1 or with mutations disrupting interactions between STIM1-CC1 and SOAR, we showed that 2-APB can inhibit SOCE independently of its effects on STIM1 puncta. Therefore, the inhibition on SOCE by 2-APB was not affected by abolishing its effect on the coupling between STIM1-CC1 and SOAR (Fig. 2a–c). We further examined this phenomenon using constructs based on the SOAR molecule as opposed to intact STIM1. First, we examined the effects of 2-APB on constitutive Ca^{2+} influx in HEK Orai1 cells co-expressing SOAR-L416G. The SOAR-L416G molecule has a compromised CC1-docking region, and its L416 residue, critical for CC1-SOAR interaction, is mutated to a non-functional glycine and is thereby devoid of inhibition by 2-APB. Similar to cells co-expressing Orai1 and wild-type SOAR [14, 51], 2-APB did not appear to physically uncouple SOAR-L416G and Orai1 as there was no decrease in FRET signals. Instead, we observed that 2-APB enhanced the FRET signals between Orai1 and SOAR-L416G (Fig. 2f, left trace). Moreover, even with its inhibitory effect on SOAR missing, 2-APB could still greatly inhibit the constitutive Ca^{2+} entry (Fig. 2f, right trace). Second, we checked the effects of 2-APB on Orai1-SS, a construct with one Orai1 subunit fused with one SOAR (336–485) dimer [20, 60]. The SOAR dimer also does not have the CC1 region that is critical for the binding of SOAR, and it is unable to form heteromers with the CC1 region of native STIM1 [24], thus it cannot be inhibited by 2-APB. We observed that 2-APB similarly inhibited the constitutive Ca^{2+} influx in HEK cells overexpressing Orai1-SS, Orai1-SS-ΔN1 (Δ1–73), or Orai1-SS-ΔC1 (Δ277–301) [60] (Fig. 2g). Taken together, after the removal of 2-APB's inhibition sites, 2-APB can still inhibit constitutive Ca^{2+} entry induced by these STIM1 mutants. Therefore, 2-APB's inhibitory effect on STIM1, or its enhancing effect on the coupling between STIM1-CC1 and SOAR, is not essential for the inhibition of Ca^{2+} influx through STIM1-activated Orai1 channels. In other words, 2-APB can inhibit SOCE through sites other than those identified in the STIM1 molecule.

2-APB modifies Ca^{2+} entry mediated by constitutively active Orai1 mutants, independently of STIM1

Since SOCE is mediated by both STIM1 and Orai1, the inhibition of SOCE by 2-APB could occur at the level of STIM1, Orai1, or STIM1-Orai1 coupling. With 2-APB's inhibitory sites on STIM1 identified and their non-essential role in the inhibition of SOCE established, we then examined possible actions of 2-APB on Orai1 channels. Normally, Orai1 channels are inactive at rest (Fig. 3a), and they become active through the coupling of STIM1. Thus, it is not possible to dissect the inhibitory actions of 2-APB on wt Orai1 in a STIM1-free background. However, there have been identified Orai1 mutants that are constitutively active even without the coupling of STIM1 [28, 33, 34]. These mutants make it possible for the direct assessment of 2-APB's effect on Orai1 channels.

Initially, we examined the effects of 2-APB on the Ca^{2+} entry mediated by constitutive Ca^{2+} influx through the Orai1-P245T mutant [33] and revealed that it was also inhibited by 2-APB (Fig. 3b). Similarly, Ca^{2+} entry via the Orai1-V102A mutant [28] was also inhibited by 2-APB (Fig. 3c). Moreover, this inhibition was unaffected by either co-expression of STIM1 or deletion of the Orai1 c-terminus (267–301) to abolish its ability to bind STIM1 [60] (Fig. 3c). Thus, this inhibition is independent of STIM1, indicating a direct inhibition on Orai1 channels.

Interestingly, 2-APB totally lost its ability to inhibit Ca^{2+} entry through a different V102 mutant, Orai1-V102C [28] (Fig. 3d, e). In HEK cells stably expressing Orai1-V102C, the resulting constitutive Ca^{2+} entry (Fig. 3d) or whole-cell current (Fig. 3e) was transiently enhanced by 2-APB. Similar enhancing effects were seen in cells co-expressing STIM1 and Orai1-V012C or in cells expressing Orai1-V102C-ΔC2, a mutant that loses its ability to bind STIM [60] (Fig. 3f).

2-APB's actions on STIM1 contributes to its inhibition on SOCE

When not bound with STIM1, constitutively active Orai1-V102C was not inhibited by 2-APB (Fig. 3d–f), making it a perfect tool to dissect possible inhibition of 2-APB on STIM1-Orai1 coupling. We thus examined the effects of 2-APB on Orai1-V102C that were coupled with STIM1. After store depletion, SOCE mediated by STIM1 and wt Orai1 was first transiently activated, then rapidly inhibited by 2-APB [19, 25] (Fig. 4a). In cells co-expressing Orai1-V012C and STIM1, when examined with Ca^{2+} imaging, the transient activation phase on SOCE was greatly enhanced and prolonged. The inhibitory effect by 2-APB was not easily visible (Fig. 4b). However, a slight inhibition of I_{CRAC} could be seen when measured with whole-cell patch clamp, a more accurate method to assess SOCE (Fig. 4c). After approximately 4 min in 2-APB, the removal of 2-APB induced an immediate increase in whole-cell current, indicating an inhibition around 25 % (Fig. 4c). However, there was no such effect in HEK Orai1-V102C cells with fully filled stores (Fig. 3e). Therefore, after store depletion, the binding of STIM1 to Orai1-V102C makes it susceptible to the inhibition by 2-APB.

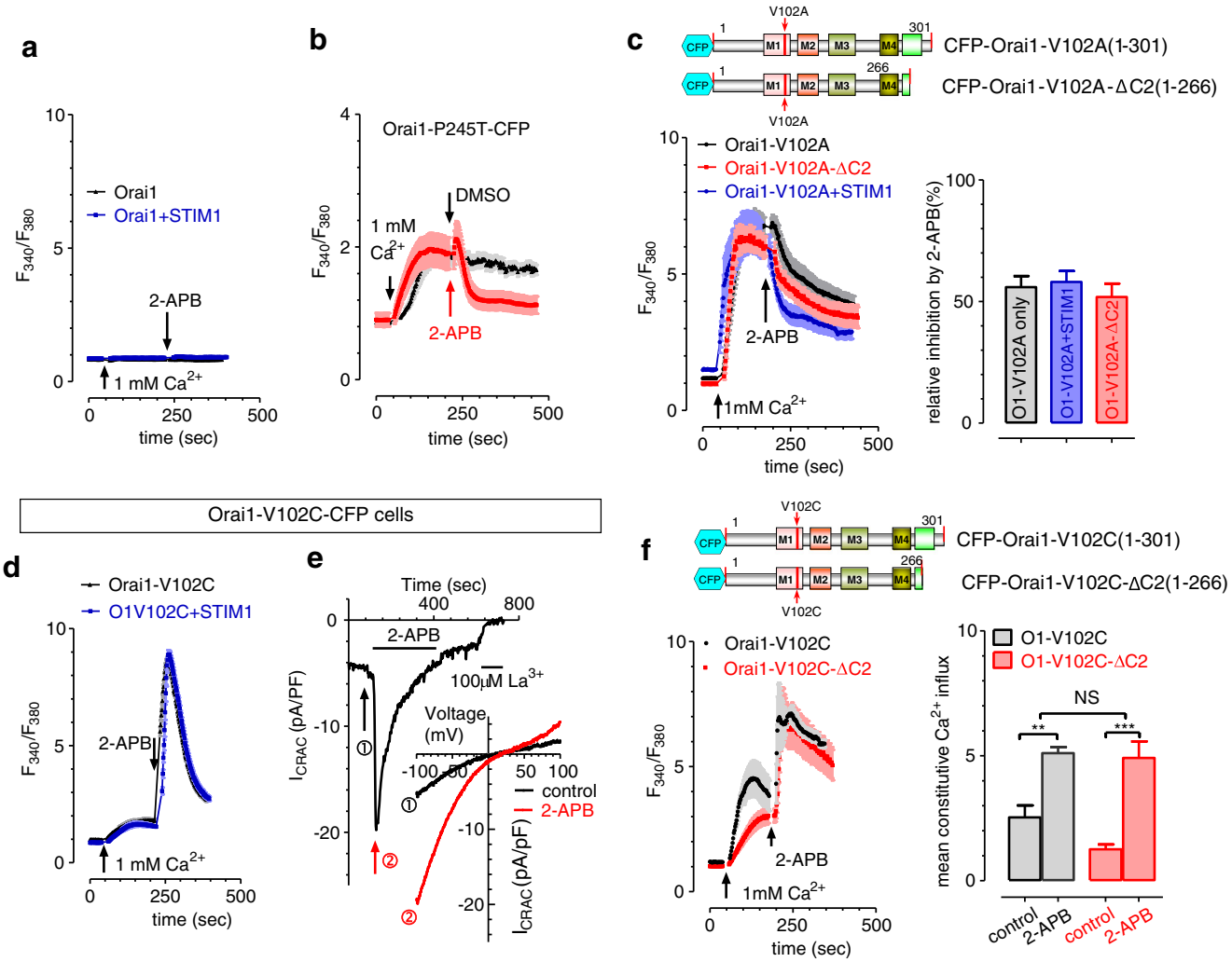

Fig. 3 2-APB can directly enhance or inhibit constitutive Ca^{2+} influx that are mediated by Orai1 mutants. Intracellular Ca^{2+} signals were measured with Fura-2. All 2-APB (50 μM) treatments were conducted when ER Ca^{2+} store were full. **a** 2-APB did not induce Ca^{2+} entry in HEK Orai1 or STIM1-Orai1 stable cells (n = 3). **b** Compared to DMSO controls, in HEK cells transiently expressing Orai1-P245T-CFP, constitutive Ca^{2+} influxes mediated by Orai1-P245T were greatly inhibited by 2-APB (34.7 ± 5.3 %, $p < 0.001$, t test, n = 3). **c** Compared to DMSO controls, in HEK wt cells transiently expressing Orai1-V102A, Orai1-V102A together with STIM1, or Orai1-V102A-ΔC2 (Δ267–301), 2-APB similarly inhibited constitutive Ca^{2+} entry through Orai1-V102A. *Left*, representative curve; *right*, statistics ($p < 0.001$ for all three groups, n = 3, t test). **d** In HEK Orai1-V102C-CFP cells, constitutive Ca^{2+} influxes mediated by Orai1-V102C were greatly enhanced by 2-APB. Overexpression of STIM1-YFP has no effect on constitutive or 2-APB-induced Ca^{2+} entry (n = 4, paired t test, $p > 0.65$). These two types of cells were seeded on the same coverslip, and fura-2 signals were measured simultaneously. **e** In HEK Orai1-V102C cells, 2-APB enhanced whole cell current from 2.6 ± 0.7 pA/pF to currents with a peak of 15.0 ± 3.5 pA/pF (p = 0.008, paired t test, n = 6). *Insert*: typical I-V relationship measured at time points indicated by *arrows*. To avoid passive store depletion, pipette solution contained 100 nM free Ca^{2+} and 2 mM ATP. **f** 2-APB enhanced constitutive Ca^{2+} influxes similarly in HEK wt cells transiently expressing Orai1-V102C or its mutant devoid of STIM1 binding, Orai1-Δ(267–301) (n = 3, $p < 0.003$, t test). There was no difference in maximal APB-induced responses between these two groups (n = 3, $p > 0.87$, t test)

This inhibition on STIM1-bound Orai1-V102C could either be induced by 2-APB's effects at the level of STIM1 or on the coupling between STIM1 and Orai1-V102C. We first tried to check 2-APB's effects in cells co-expressing Orai1-V102C together with various constitutively active, full-length STIM1 mutants. Our attempt failed as cells co-expressing both proteins all died, probably due to the toxic effect induced by high cytosolic Ca^{2+} levels. We then examined the effect of 2-APB in HEK cells co-expressing Orai1-V102C and SOAR-L416G, a mutant that is devoid of 2-APB's inhibition on STIM1. The constitutive Ca^{2+} entry mediated by Orai1-V102C and SOAR-L416G was not affected by 2-APB even after 5 min incubation (Fig. 4d). This result indicates that 2-APB's actions on STIM1-CC1 and SOAR are essential for its inhibition on STIM1-bound Orai1-V102C.

To gain some insights regarding how this enhanced coupling between STIM1-CC1 and SOAR could inhibit Ca^{2+} entry through STIM1-bound Orai1-V102C, we checked

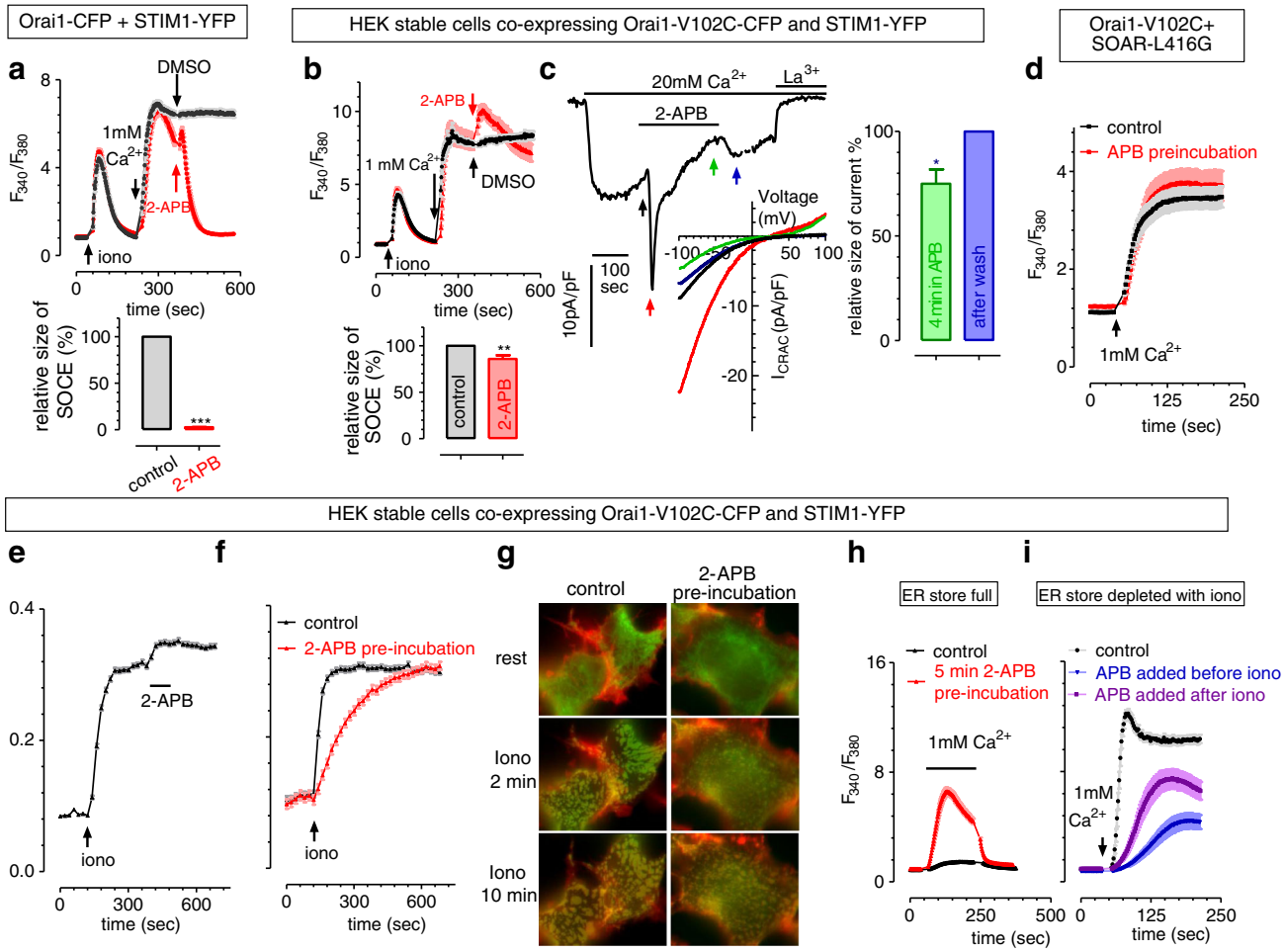

Fig. 4 2-APB-induced inhibition of STIM1 also slowly contributes to its inhibitory effect on SOCE. Unless specified, all other experiments were carried out in HEK stable cells co-expressing Orai1-V102C-CFP and STIM1-YFP. And ER Ca^{2+} store were depleted with 2.5 μM ionomycin in all imaging experiments. Intracellular Ca^{2+} levels were shown as Fura-2 ratio signals. Concentration of 2-APB was 50 μM. **a** In HEK stable cells co-expressing STIM1-YFP and Orai1-CFP, after a transient activation, 2-APB quickly inhibited SOCE mediated by STIM1 and Orai1. *Upper image*, typical traces; *lower image*, statistics showing the size of APB responses relative to DMSO controls (*t* test, $p < 0.001$, $n = 3$). **b** In HEK STIM1 + Orai1-V102C stable cells, ionomycin-induced Ca^{2+} entry was transiently enhanced by 2-APB, while the effect of inhibitions was minimal. *Upper image*, representative traces; *lower image*, statistics showing the size of APB responses relative to DMSO controls (*t* test, $p = 0.009$, $n = 3$). **c** 2-APB first transiently enhanced I_{CRAC} mediated by STIM1 and Orai1-V102C, and then it slowly inhibited I_{CRAC}. *Left*, development of whole-cell current in a typical cell; *middle*, I-V relationships of the same cell in the left figure at various time points as indicated by *arrows*. ER Ca^{2+} store in patched cells was passively depleted by including 20 mM EGTA in pipette solution. *Right*, statistics showing the recovery of current after the removal of 2-APB from bath solution. Currents in the presence of 2-APB (indicated by *green arrow*) were normalized against peak current after the removal of 2-APB (indicated by *blue arrow*). ($p = 0.02$, paired *t* test, $n = 6$). **d** In HEK tsA cells transiently expressing YFP-SOAR-L416G and Orai1-V102C-CFP, 5 min of pre-incubation of 2-APB has no effect on Ca^{2+} entry mediated by these two proteins (paired *t* test, $p = 0.83$, $n = 3$). **e** 2-APB further increased FRET signals between STIM1 and Orai1-V102C after store depletion. **f** Five minutes of pre-incubation with 2-APB slowed down the rate of increase in FRET signals between STIM1 and Orai1-V102C (0.0030 ± 0.0001 vs 0.0020 ± 0.0001 ΔN-FRET/s, paired *t* test, $p < 0.001$, $n = 4$). **g** Compared to control, 5 min of pre-incubation with 2-APB slowed down the appearance of STIM1 puncta, examined with epifluorescence imaging ($n = 4$). **h** When ER Ca^{2+} store is full, 5 min of incubation with 2-APB enhanced the mean constitutive Ca^{2+} influx from 0.46 ± 0.08 (F_{340}/F_{380}) to 3.69 ± 0.30 (F_{340}/F_{380}), (paired *t* test, $p < 0.0001$, $n = 6$). **i** Compared to controls treated with DMSO, 5 min of pre-incubation with 2-APB greatly inhibited SOCE after store depletion. When 2-APB was applied before store depletion, the inhibitory effect (76.6 ± 5.2 %) is greater than those applied after store depletion (57.1 ± 5.1 %). $n = 3$, paired *t* test, $p = 0.002$. (Color figure online)

whether 2-APB affects the coupling between STIM1 and Orai1-V102C using FRET imaging. In HEK cells stably co-expressing STIM1 and Orai1-V102C, store depletion induced an increase in FRET signals between STIM1 and Orai1-V102C. This FRET signal was then further increased by 2-APB (Fig. 4e). Similar results obtained with wt Orai1 and activated STIM1 or its cytosolic fragments were also reported previously [14, 32, 51, 53]. This result indicates that 2-APB's enhancing actions on STIM1-CC1 and SOAR are not enough to break the existing coupling between STIM1 and Orai1-

V102C. We then examined whether 2-APB pre-incubation can inhibit the development of STIM1 coupling with Orai1 during the process of store depletion. Even though it did not reduce the maximal FRET signals between STIM1 and Orai1-V012C, pre-incubation with 2-APB greatly slowed down the increasing rate of FRET signals (Fig. 4f). Similarly, pre-incubation with 2-APB also greatly delayed the formation of STIM1 puncta (Fig. 4g). Overall, these results indicate that the enhanced coupling between STIM1-CC1 and SOAR induced by 2-APB was too weak to block or disrupt the physical coupling between STIM1 and Orai1-V102C (Fig. 4e–g). However, pre-incubation with 2-APB did slow down the coupling of STIM1 to Orai1-V102C (Fig. 4f, g).

Since its inhibitory effect on the coupling of STIM1 to Orai1-V102C was more detectable when 2-APB was applied before store depletion, we examined whether 2-APB could inhibit SOCE in a similar manner. Indeed, even though pre-incubation with 2-APB did not inhibit the constitutive Ca^{2+} entry when the ER Ca^{2+} store is full (Fig. 4h), it can inhibit Ca^{2+} entry through Orai1-V102C after store depletion (Fig. 4i). And if 2-APB was applied before store depletion with ionomycin, a 5-min incubation with 2-APB inhibited SOCE by 76.6 ± 3.2 %. However, if 2-APB was applied after the stores were fully depleted, its inhibition on SOCE was significantly less (57.1 ± 5.1 %, $p = 0.002$, t test) (Fig. 4i). Thus, the extent of 2-APB's inhibition on SOCE correlates with its ability to affect the coupling between STIM1 and Orai1-V012C.

From this, we conclude that 2-APB's inhibition on STIM1-bound Orai1-V102C channels is mediated by its enhanced auto-inhibition of STIM1. Its inhibitory effect on STIM1 is not strong enough to physically disrupt the coupling between the STIM1 and Orai1-V102C complex (Fig. 4e). It is very likely that this 2-APB- and STIM1-dependent inhibition is mediated through disruption of the functional coupling between STIM1 and Orai1-V012C.

The inhibition of 2-APB on STIM1-bound Orai1-V102C is abolished by the K85E mutation at the Orai1 *N*-terminus

Even though recent evidence shows that both *N*- and *C*-termini of Orai1 are involved in channel gating and coupling with STIM1 [11, 27, 34, 42, 51, 18, 36, 61], the Orai1 *C*-terminus is clearly more involved in STIM1 binding [20, 31, 32, 60] and its *N*-terminus has been shown to be important for channel function and gating by STIM1 [23, 30, 46, 60]. More specifically, the extended transmembrane Orai1 *N*-terminal (ETON, aa73–90) region has been shown to be necessary for STIM1 binding and channel gating [11, 13]. It has been argued that the K85 residue within this region mediates STIM1 gating of the channel since the Orai1-K85E mutant has slightly reduced STIM1 binding yet completely loses its ability to mediate Ca^{2+} entry [11, 27, 23], although whether STIM1 binding to this region is required for gating is presently unclear.

We therefore examined whether the K85E mutation in the ETON region could affect the inhibition of 2-APB on SOCE mediated by STIM1-bound Orai1-V102C. Similar to an earlier report [27], the double-mutant Orai1-K85E-V102C is constitutively active and has some store-dependent activity (Fig. 5a, b). As indicated by FRET measurements, STIM1 can interact with Orai1-K85E-V102C and further activate it after store depletion (Fig. 5b, c) [27]. When 2-APB was added after the application of Ca^{2+}, both the constitutive Ca^{2+} entry and SOCE through Orai1-K85E-V102C channels were greatly enhanced (Fig. 5b). When 2-APB was applied 5 min before the addition of Ca^{2+}, both constitutive Ca^{2+} influx and SOCE were still enhanced by 2-APB (Fig. 5d, e). Thus, the K85E mutation abolished 2-APB's inhibition on STIM1-bound Orai1-V102C (Fig. 5e vs Fig. 4i). Since pre-incubation with 2-APB could still slow the rate of increase in FRET signals between STIM1 and Orai1-K85E-V102C, this indicates that 2-APB's inhibitory effect on STIM1 is still intact (Fig. 5f). Therefore, K85 serves as a critical link, relaying 2-APB's inhibitory effect on STIM1 to its actions on Orai1-V102C. Thus, the ETON region is essential in mediating 2-APB's inhibition of STIM1-bound Orai1-V102C. More studies are needed to examine whether those corresponding regions in Orai2 or Orai3 also mediate 2-APB's inhibition on STIM1-bound Orai2 or Orai3.

Discussion

The store-operated Ca^{2+} signals mediated by STIM1 and STIM2 proteins and the three mammalian Orai channels are shown to be crucial in many cellular responses [29, 44, 46, 52] and to have important physiological roles and involvements in many disease states [44, 50]. There is a great need to develop highly isoform- and tissue-specific inhibitors of SOCE in order to better understand the exact physiological or pathological roles of the different isoforms of STIM and Orai and eventually for the development of disease treatments. Even under the guidance from the solved crystal structure of Orai1 and SOAR [18, 57], drug development is still at its preliminary stage, and the underlying molecular basis for most SOCE inhibitors still remains largely undefined [19, 41]. As one of the most used SOCE modifiers, 2-APB has complex effects, enhancing SOCE at low concentrations and inhibiting SOCE after a transient activation at higher concentrations [25, 39]. Its actions on CRAC activity mediated by different subtypes of STIM and Orai have been intensively examined [10, 19, 22, 25, 32, 37–39, 41, 43, 53]. However, current understandings of the molecular basis of its actions are mainly constrained to its activation of SOCE [1, 2, 4, 40, 43, 53, 55, 56], while the

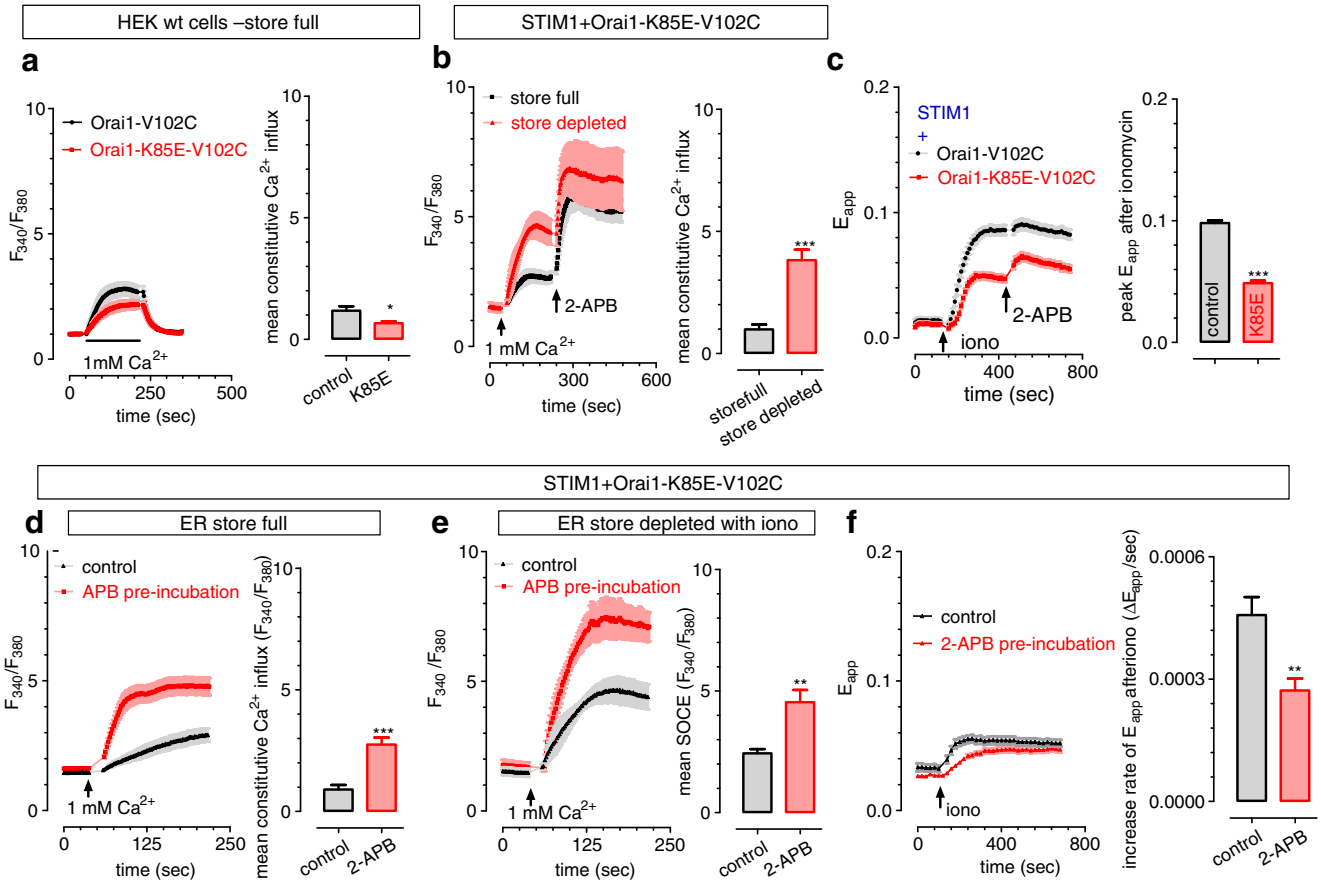

Fig. 5 The Orai1 K85E mutation abolished 2-APB's inhibition on STIM1-bound Orai1-V102C. Except for the first figure, all other experiments were carried out in HEK SITM1-YFP stable cells transiently expressing Orai1-V102C-CFP, or its K85E mutant. Ionomycin (2.5 μM) was used for store depletion, and the effects of 2-APB (50 μM) were examined. Intracellular Ca^{2+} levels were examined with Fura-2. For each sub-figure, typical traces are shown on the *left* and statistics are shown on the *right*. $n = 3$, paired t test. $^{***}p < 0.0003$; $^{**}p < 0.006$, $^{*}p < 0.05$. **a** When transiently expressed in HEK wt cells, K85E mutation (*red trace*) decreases the resulting constitutive Ca^{2+} entry as compared to control (*black trace*). **b** When applied after the addition of Ca^{2+}, 2-APB enhanced the Ca^{2+} responses mediated by Orai1-K85E-V102C, regardless of whether the ER store is full (*black trace*) or depleted (*red trace*). **c** Compared to control (*black trace*), K85E mutation (*red trace*) reduced ionomycin-induced increases in FRET signals between STIM1 and Orai1-V102C. **d**–**f** When 2-APB is applied 5 min before store depletion with ionomycin, both **d** constitutive Ca^{2+} entry and **e** SOCE were enhanced, **f** while the rate of ionomycin-induced increase in FRET signals between STIM1 and Orai1-K85E-V102C was significantly slowed

possible mechanisms of its inhibitory effects are poorly understood [19, 38, 41].

The results here reveal that 2-APB could inhibit SOCE by directly affecting the two essential mediators of SOCE, STIM1, and Orai1. The geometry of the Orai1 pore is critical for the direct inhibition of 2-APB, and its fast-developing inhibition on Orai1 channels is 90 % complete within 90 s (Fig. 3b, c). 2-APB's direct inhibition on STIM1 fully develops within several minutes (Fig. 1h). 2-APB inhibits STIM1 by enhancing or inducing coupling between its CC1 and SOAR region, thus locking STIM1 to its auto-inhibitory, resting state. Aside from its direct actions on Orai1 and STIM1, 2-APB can also indirectly inhibit the functional coupling between STIM1 and Orai1 via its actions on STIM1. This STIM1-dependent, indirect effect develops slower than 2-APB's direct actions on STIM1 (Fig. 1h vs Fig. 4c, i). This slower action is probably caused by the enhanced coupling between Orai1 and STIM1 or STIM1ct [32, 53] (Fig. 4e).

Using the constitutively active Orai1-P245L mutant, we demonstrate that 2-APB (50 μM) has direct dual effects on open Orai1 channels: a transient potentiation followed by an inhibition (Fig. 3b). While this potentiation may be caused by dilating the open Orai1 channel pore [54], the molecular mechanisms underlying the direct inhibition by 2-APB are still unclear. We showed that the excitatory and inhibitory effect of 2-APB can be separated by point mutations on the V102 residue. 2-APB can directly activate, but cannot inhibit, the V102C mutant (Fig. 3d–f) [28]. In contrast, 2-APB can directly inhibit but cannot enhance the V102A-mediated Ca^{2+} entry (Fig. 3c). This lack of enhancement may be caused by the large pore of the V102A. Its pore can pass Ca^{2+} ions without any steric hindrance [54], thus 2-APB cannot enhance

Ca^{2+} entry through the V012A channels by further dilating its pore (Fig. 3c) [54]. While the pore size of V102C falls between that of wild type and V102A [28, 54], thus the APB-induced dilation of its pore will greatly potentiate Ca^{2+} current through V102C (Fig. 3d–f). This APB-induced large potentiation on Orai1-V102C channels (5~10-fold increase, Fig. 3e and Fig. 4h) may mask 2-APB's weak inhibitory effect on open Orai1 channels (30~50 % inhibition, Fig. 3b, c), resulting in no inhibition of Orai1-V102C by 2-APB. When measured with Ca^{2+} imaging or whole-cell patch clamp, 2-APB's activation on Orai1-V102C may appear "transient" (Fig. 3d, e), and the activation may terminate in 6 min (Fig. 3d). This transient activation on Orai1-V102C may be an artifact caused by Ca^{2+}-dependent inactivation (CDI). Our data clearly showed that 2-APB's activation of Orai1-V102C is still intact after a 5-min incubation with 50 μM 2-APB in Ca^{2+}-free solution (Fig. 4h). Nevertheless, for STIM1-free Orai1-V102C, this transient activation (Fig. 3d, e) is clearly not caused by some slowly developing inhibition on Orai1, as there is no increase in I_{CRAC} after the removal of 2-APB (Fig. 3e). By contrast, for STIM1-bound Orai1-V102C, there is clearly a recovery of I_{CRAC} after the removal of 2-APB (Fig. 4c). Collectively, 2-APB's activation on Orai1-V012C is long lasting, which could help further dissection of STIM1-dependent inhibition on open Orai1 channels.

Store depletion leads to the formation of STIM1 puncta and the physical coupling of STIM1 to Orai1. There has been some controversy on 2-APB's ability to inhibit STIM1 puncta [10, 32, 38, 59]. STIM1 puncta transiently expressed in HEK wt cells were shown to be greatly inhibited by 2-APB [10, 38]. There were also reports showing that, in HEK cells expressing STIM1 together with Orai1, 2-APB's ability to inhibit STIM1 puncta is either severely impaired or abolished [10, 32, 59]. It is still unclear whether this discrepancy is an Orai1 effect or not. By imaging STIM1 cells with or without co-expression of Orai1 in the same view field, we demonstrate that most of this discrepancy is caused by the differences in the amount of Orai1 used in different labs (Fig. 2d): co-expression of Orai1 together with STIM1 abolishes 2-APB's ability to inhibit STIM1 puncta. Based on this observation and previous reports [10, 32, 38, 51, 59], we propose a model to explain whether STIM1 puncta can be inhibited by 2-APB or not. Thus, 2-APB has two antagonizing, "push and pull" effects on STIM1: its direct actions on the CC1 and SOAR region of STIM1 will pull the STIM1-SOAR region back toward ER to lock STIM1 in its resting state, thereby inhibiting the formation of STIM1 puncta [10, 38], while its Orai1-dependent enhancing effects on the coupling between STIM1 and Orai1 [32, 51, 53, 59] will push the STIM1-SOAR region toward the PM, keeping STIM1 in its activated, punctate distribution (Fig. 2d). The Orai1-dependent pushing effect of 2-APB is stronger than its pulling effect on STIM1, thus 2-APB cannot disrupt established STIM1-Orai1 interactions. Instead, it enhances FRET signals between Orai1 and STIM1 or STIM1 fragments [32, 51, 53] (Fig. 4e).

Overall, those puncta formed by Orai1-bound STIM1 are resistant to 2-APB, while Orai1-free STIM1 puncta can be abolished by 2-APB. Thus, according to this model, the ability of 2-APB to inhibit wt STIM1 puncta depends on the relative amount of STIM1 that is not bound to Orai1. In HEK wt cells overexpressing STIM1, endogenous Orai1 can only keep a limited amount of STIM1 molecules in their punctate distributions. The majority of punctate areas are formed by Orai1-free STIM1 and thus can be abolished by 2-APB (Fig. 2a). As a result, 2-APB can reduce STIM1 puncta in HEK STIM1 cells. When a moderate amount of Orai1 is also co-expressed with STIM1, most STIM1 will be bound to Orai1 after store depletion. Thus, only a small portion of STIM1 molecules are not bound with Orai1 and these puncta can be abolished by 2-APB, resulting in partial inhibition of STIM1 puncta. Therefore, the extent of 2-APB inhibition is dependent on relative expression levels of Orai proteins. Indeed, there was one report showing that the expression level of Orai proteins is inversely related to 2-APB's ability to reduce STIM1 puncta [10]. Thus, if enough Orai1 is expressed, after store depletion, all STIM1 molecules would be bound with Orai1, and this powerful Orai1-pushing effect of 2-APB would completely override its inhibition of STIM1 puncta (Fig. 2d) [59].

It has been reported that Orai1 has two STIM1-binding sites [18, 36, 61], with its *N*-terminus proposed for channel gating, and its *C*-terminus for STIM1 binding [16, 23, 60]. Recent evidence suggests that both termini of Orai1 are involved in STIM1-induced channel gating [11, 27]. It was proposed that 2-APB might compete with STIM1 to gate Orai3 channels [56]. Consistent with this idea, 2-APB-activated Ca^{2+} influx through Orai1-K85E-V102C is similar to that mediated by STIM1-bound Orai1-K85E-V102C (red trace in Fig. 5d vs black trace in Fig. 5e). Moreover, we show that pre-incubation with 2-APB could further increase Ca^{2+} influx through STIM1-bound Orai1-K85E-V102C (Fig. 5e). And this increase in SOCE activity does not seem to come from alterations in STIM1 binding, as the maximal FRET signals between STIM1 and Orai1-K85E-V102C was unaffected (Fig. 5f). Thus, this result indicates that there might be a distinct gating residue in Orai1 channels, but the location of this site, that is, whether it is at the *C*- or *N*-terminus, is not clear. Further studies are needed to validate this possibility.

The appearance of STIM1 puncta can reliably indicate the activation of STIM1 [17, 21], thus making STIM1 puncta a very good tool for examining the activation of STIM1 and the developing of STIM1 inhibitors. However, the quantification of STIM1 puncta is difficult [15]. Regular epifluorescent images of STIM1 puncta are often blurred by fluorescence contaminations from out-of-focus signals, thus making it even more difficult to quantify (Fig. 2a vs Fig. 2d). In addition, to

obtain confocal or TIRF measurements of STIM1 puncta, expensive equipment and much training are required. These drawbacks limit the use of STIM1 puncta to monitor STIM1 activation. Here, we show that these abovementioned limitations could be overcome by our recently developed two-component system, which consists of STIM1-(1–310)-CFP and YFP-SOAR or YFP-SOAR-5KQ [24]. The activation status of STIM1 can now be easily measured with co-localization or FRET signals between the two components, making the assessment of drug effects fast and precise (Fig. 1h).

In summary, we adopt here a two-component FRET assay to dissect the effects of pharmacological tools on STIM1 activation. With this tool and other approaches, we have evaluated different inhibitory effects of 2-APB at the levels of STIM1, Orai1, and the coupling between these two proteins. Our findings further clarify the molecular basis underlying 2-APB's actions on SOCE. These strategies can be further extended to examine whether similar molecular mechanisms are adaptable to Orai2 and Orai3 and to dissect the mechanisms of action of other SOCE inhibitors, particularly the recently developed 2-APB analogs [14]. Thus, our results provide a solid base for better understanding of SOCE activation, as well as the design of enhanced pharmacological tools or drug candidates targeting SOCE to treat human disorders associated with aberrant Ca^{2+} entry and homeostasis.

Acknowledgments We thank Dr. Yubin Zhou at Texas A&M University Health Science Center for his valuable discussion and insightful suggestions. We thank Dr. Tao Xu and Dr. Pingyong Xu for sharing with us the Orai1-S-S construct. This work was supported by the National Institutes of Health grants (AI058173 and GM109279 to DLG), the National Natural Science foundation of China (NSFC-31471279 to Y.W.), the Recruitment Program for Young Professionals of China (to Y.W.), the Program for New Century Excellent Talents in University (NCET-13-0061 to Y.W.), and the American Heart Association Scientist Development Grant (13SDG17200006 to S.L.Z.).

Authors' contribution DLG and YW supervised and coordinated the study. SLZ provided Orai1-SS deletion mutants and intellectual inputs to the study. LH, GM, and YZ designed and generated some plasmid constructs. MW, AS, LZ, and YW performed confocal, calcium, FRET, and epifluorescence imaging. YW carried out the whole-cell patching. JL provided tech support for cell culture and confocal imaging. MW, AS, LZ, YW, and YZ analyzed data, with inputs from the other authors. SZ and SLZ helped with manuscript writing. YZ, YW, and DLG wrote the manuscript.

References

1. Amcheslavsky A, Safrina O, Cahalan MD (2013) Orai3 TM3 point mutation G158C alters kinetics of 2-APB-induced gating by disulfide bridge formation with TM2 C101. J Gen Physiol 142:405–412
2. Amcheslavsky A, Safrina O, Cahalan MD (2014) State-dependent block of Orai3 TM1 and TM3 cysteine mutants: insights into 2-APB activation. J Gen Physiol 143:621–631
3. Bergmeier W, Weidinger C, Zee I, Feske S (2013) Emerging roles of store-operated Ca(2)(+) entry through STIM and ORAI proteins in immunity, hemostasis and cancer. Channels (Austin) 7:379–391
4. Bergsmann J, Derler I, Muik M, Frischauf I, Fahrner M, Pollheimer P, Schwarzinger C, Gruber HJ, Groschner K, Romanin C (2011) Molecular determinants within N terminus of Orai3 protein that control channel activation and gating. J Biol Chem 286:31565–31575
5. Berridge MJ, Lipp P, Bootman MD (2000) The versatility and universality of calcium signalling. Nat Rev Mol Cell Biol 1:11–21
6. Boussif O, Lezoualc'h F, Zanta MA, Mergny MD, Scherman D, Demeneix B, Behr JP (1995) A versatile vector for gene and oligonucleotide transfer into cells in culture and in vivo: polyethylenimine. Proc Natl Acad Sci U S A 92:7297–7301
7. Carrasco S, Meyer T (2011) STIM proteins and the endoplasmic reticulum-plasma membrane junctions. Annu Rev Biochem 80:973–1000
8. Clapham DE (1995) Calcium signaling. Cell 80:259–268
9. Covington ED, Wu MM, Lewis RS (2010) Essential role for the CRAC activation domain in store-dependent oligomerization of STIM1. Mol Biol Cell 21:1897–1907
10. DeHaven WI, Smyth JT, Boyles RR, Bird GS, Putney JW Jr (2008) Complex actions of 2-aminoethyldiphenyl borate on store-operated calcium entry. J Biol Chem 283:19265–19273
11. Derler I, Plenk P, Fahrner M, Muik M, Jardin I, Schindl R, Gruber HJ, Groschner K, Romanin C (2013) The extended transmembrane Orai1 N-terminal (ETON) region combines binding interface and gate for Orai1 activation by STIM1. J Biol Chem 288:29025–29034
12. Fahrner M, Muik M, Schindl R, Butorac C, Stathopulos P, Zheng L, Jardin I, Ikura M, Romanin C (2014) A coiled-coil clamp controls both conformation and clustering of stromal interaction molecule 1 (STIM1). J Biol Chem 289:33231–33244
13. Gudlur A, Quintana A, Zhou Y, Hirve N, Mahapatra S, Hogan PG (2014) STIM1 triggers a gating rearrangement at the extracellular mouth of the ORAI1 channel. Nat Commun 5:5164
14. Hendron E, Wang X, Zhou Y, Cai X, Goto J, Mikoshiba K, Baba Y, Kurosaki T, Wang Y, Gill DL (2014) Potent functional uncoupling between STIM1 and Orai1 by dimeric 2-aminodiphenyl borinate analogs. Cell Calcium 56:482–492
15. Hewavitharana T, Deng X, Wang Y, Ritchie MF, Girish GV, Soboloff J, Gill DL (2008) Location and function of STIM1 in the activation of Ca2+ entry signals. J Biol Chem 283:26252–26262
16. Hogan PG, Lewis RS, Rao A (2010) Molecular basis of calcium signaling in lymphocytes: STIM and ORAI. Annu Rev Immunol 28:491–533
17. Hogan PG, Rao A (2015) Store-operated calcium entry: mechanisms and modulation. Biochem Biophys Res Commun 460:40–49
18. Hou X, Pedi L, Diver MM, Long SB (2012) Crystal structure of the calcium release-activated calcium channel Orai. Science 338:1308–1313
19. Jairaman A, Prakriya M (2013) Molecular pharmacology of store-operated CRAC channels. Channels (Austin) 7:402–414
20. Li Z, Liu L, Deng Y, Ji W, Du W, Xu P, Chen L, Xu T (2011) Graded activation of CRAC channel by binding of different numbers of STIM1 to Orai1 subunits. Cell Res 21:305–315
21. Liou J, Kim ML, Heo WD, Jones JT, Myers JW, Ferrell JE Jr, Meyer T (2005) STIM is a Ca2+ sensor essential for Ca2+-store-depletion-triggered Ca2+ influx. Curr Biol 15:1235–1241
22. Lis A, Peinelt C, Beck A, Parvez S, Monteilh-Zoller M, Fleig A, Penner R (2007) CRACM1, CRACM2, and CRACM3 are store-operated Ca2+ channels with distinct functional properties. Curr Biol 17:794–800
23. Lis A, Zierler S, Peinelt C, Fleig A, Penner R (2010) A single lysine in the N-terminal region of store-operated channels is critical for STIM1-mediated gating. J Gen Physiol 136:673–686

24. Ma G, Wei M, He L, Liu C, Wu B, Zhang SL, Jing J, Liang X, Senes A, Tan P, Li S, Sun A, Bi Y, Zhong L, Si H, Shen Y, Li M, Lee MS, Zhou W, Wang J, Wang Y, Zhou Y (2015) Inside-out Ca(2+) signalling prompted by STIM1 conformational switch. Nat Commun 6:7826
25. Ma HT, Venkatachalam K, Parys JB, Gill DL (2002) Modification of store-operated channel coupling and inositol trisphosphate receptor function by 2-aminoethoxydiphenyl borate in DT40 lymphocytes. J Biol Chem 277:6915–6922
26. Mancarella S, Wang Y, Gill DL (2009) Calcium signals: STIM dynamics mediate spatially unique oscillations. Curr Biol 19: R950–R952
27. McNally BA, Somasundaram A, Jairaman A, Yamashita M, Prakriya M (2013) The C- and N-terminal STIM1 binding sites on Orai1 are required for both trapping and gating CRAC channels. J Physiol 591:2833–2850
28. McNally BA, Somasundaram A, Yamashita M, Prakriya M (2012) Gated regulation of CRAC channel ion selectivity by STIM1. Nature 482:241–245
29. Moccia F, Zuccolo E, Soda T, Tanzi F, Guerra G, Mapelli L, Lodola F, D'Angelo E (2015) Stim and Orai proteins in neuronal Ca(2+) signaling and excitability. Front Cell Neurosci 9:153
30. Muik M, Fahrner M, Schindl R, Stathopulos P, Frischauf I, Derler I, Plenk P, Lackner B, Groschner K, Ikura M, Romanin C (2011) STIM1 couples to ORAI1 via an intramolecular transition into an extended conformation. EMBO J 30:1678–1689
31. Muik M, Frischauf I, Derler I, Fahrner M, Bergsmann J, Eder P, Schindl R, Hesch C, Polzinger B, Fritsch R, Kahr H, Madl J, Gruber H, Groschner K, Romanin C (2008) Dynamic coupling of the putative coiled-coil domain of ORAI1 with STIM1 mediates ORAI1 channel activation. J Biol Chem 283:8014–8022
32. Navarro-Borelly L, Somasundaram A, Yamashita M, Ren D, Miller RJ, Prakriya M (2008) STIM1-Orai1 interactions and Orai1 conformational changes revealed by live-cell FRET microscopy. J Physiol 586:5383–5401
33. Nesin V, Wiley G, Kousi M, Ong EC, Lehmann T, Nicholl DJ, Suri M, Shahrizaila N, Katsanis N, Gaffney PM, Wierenga KJ, Tsiokas L (2014) Activating mutations in STIM1 and ORAI1 cause overlapping syndromes of tubular myopathy and congenital miosis. Proc Natl Acad Sci U S A 111:4197–4202
34. Palty R, Stanley C, Isacoff EY (2015) Critical role for Orai1 C-terminal domain and TM4 in CRAC channel gating. Cell Res 25: 963–980
35. Parekh AB, Putney JW Jr (2005) Store-operated calcium channels. Physiol Rev 85:757–810
36. Park CY, Hoover PJ, Mullins FM, Bachhawat P, Covington ED, Raunser S, Walz T, Garcia KC, Dolmetsch RE, Lewis RS (2009) STIM1 clusters and activates CRAC channels via direct binding of a cytosolic domain to Orai1. Cell 136:876–890
37. Parvez S, Beck A, Peinelt C, Soboloff J, Lis A, Monteilh-Zoller M, Gill DL, Fleig A, Penner R (2008) STIM2 protein mediates distinct store-dependent and store-independent modes of CRAC channel activation. FASEB J 22:752–761
38. Peinelt C, Lis A, Beck A, Fleig A, Penner R (2008) 2-Aminoethoxydiphenyl borate directly facilitates and indirectly inhibits STIM1-dependent gating of CRAC channels. J Physiol 586: 3061–3073
39. Prakriya M, Lewis RS (2001) Potentiation and inhibition of Ca(2+) release-activated Ca(2+) channels by 2-aminoethyldiphenyl borate (2-APB) occurs independently of IP(3) receptors. J Physiol 536:3–19
40. Prakriya M, Lewis RS (2006) Regulation of CRAC channel activity by recruitment of silent channels to a high open-probability gating mode. J Gen Physiol 128:373–386
41. Putney JW (2010) Pharmacology of store-operated calcium channels. Mol Interv 10:209–218
42. Rothberg BS, Wang Y, Gill DL (2013) Orai channel pore properties and gating by STIM: implications from the Orai crystal structure. Sci Signal 6:pe9
43. Schindl R, Bergsmann J, Frischauf I, Derler I, Fahrner M, Muik M, Fritsch R, Groschner K, Romanin C (2008) 2-aminoethoxydiphenyl borate alters selectivity of Orai3 channels by increasing their pore size. J Biol Chem 283:20261–20267
44. Shaw PJ, Feske S (2012) Regulation of lymphocyte function by ORAI and STIM proteins in infection and autoimmunity. J Physiol 590:4157–4167
45. Shim AH, Tirado-Lee L, Prakriya M (2015) Structural and functional mechanisms of CRAC channel regulation. J Mol Biol 427: 77–93
46. Soboloff J, Rothberg BS, Madesh M, Gill DL (2012) STIM proteins: dynamic calcium signal transducers. Nat Rev Mol Cell Biol 13:549–565
47. Stathopulos PB, Zheng L, Li GY, Plevin MJ, Ikura M (2008) Structural and mechanistic insights into STIM1-mediated initiation of store-operated calcium entry. Cell 135:110–122
48. Tian C, Du L, Zhou Y, Li M (2016) Store-operated CRAC channel inhibitors: opportunities and challenges. Future Med Chem 8:817–832
49. Trebak M (2012) STIM/Orai signalling complexes in vascular smooth muscle. J Physiol 590:4201–4208
50. Vashisht A, Trebak M, Motiani RK (2015) STIM and Orai proteins as novel targets for cancer therapy. Am J Physiol Cell Physiol. doi:10.1152/ajpcell.00064.2015
51. Wang X, Wang Y, Zhou Y, Hendron E, Mancarella S, Andrake MD, Rothberg BS, Soboloff J, Gill DL (2014) Distinct Orai-coupling domains in STIM1 and STIM2 define the Orai-activating site. Nat Commun 5:3183
52. Wang Y, Deng X, Hewavitharana T, Soboloff J, Gill DL (2008) Stim, ORAI and TRPC channels in the control of calcium entry signals in smooth muscle. Clin Exp Pharmacol Physiol 35:1127–1133
53. Wang Y, Deng X, Zhou Y, Hendron E, Mancarella S, Ritchie MF, Tang XD, Baba Y, Kurosaki T, Mori Y, Soboloff J, Gill DL (2009) STIM protein coupling in the activation of Orai channels. Proc Natl Acad Sci U S A 106:7391–7396
54. Xu X, Ali S, Li Y, Yu H, Zhang M, Lu J, Xu T (2016) 2-Aminoethoxydiphenyl borate potentiates CRAC current by directly dilating the pore of open Orai1. Sci Rep 6:29304
55. Yamashita M, Prakriya M (2014) Divergence of Ca(2+) selectivity and equilibrium Ca(2+) blockade in a Ca(2+) release-activated Ca(2+) channel. J Gen Physiol 143:325–343
56. Yamashita M, Somasundaram A, Prakriya M (2011) Competitive modulation of Ca2+ release-activated Ca2+ channel gating by STIM1 and 2-aminoethyldiphenyl borate. J Biol Chem 286:9429–9442
57. Yang X, Jin H, Cai X, Li S, Shen Y (2012) Structural and mechanistic insights into the activation of stromal interaction molecule 1 (STIM1). Proc Natl Acad Sci U S A 109:5657–5662
58. Zal T, Gascoigne NR (2004) Photobleaching-corrected FRET efficiency imaging of live cells. Biophys J 86:3923–3939
59. Zeng B, Chen GL, Xu SZ (2012) Store-independent pathways for cytosolic STIM1 clustering in the regulation of store-operated Ca(2+) influx. Biochem Pharmacol 84:1024–1035
60. Zheng H, Zhou MH, Hu C, Kuo E, Peng X, Hu J, Kuo L, Zhang SL (2013) Differential roles of the C and N termini of Orai1 protein in interacting with stromal interaction molecule 1 (STIM1) for Ca2+ release-activated Ca2+ (CRAC) channel activation. J Biol Chem 288:11263–11272
61. Zhou Y, Meraner P, Kwon HT, Machnes D, Oh-hora M, Zimmer J, Huang Y, Stura A, Rao A, Hogan PG (2010) STIM1 gates the store-operated calcium channel ORAI1 in vitro. Nat Struct Mol Biol 17: 112–116